

Stability against freezing of aqueous solutions on early Mars

Alberto G. Fairén¹, Alfonso F. Davila¹, Luis Gago-Duport², Ricardo Amils^{3,4} & Christopher P. McKay¹

Many features of the Martian landscape are thought to have been formed by liquid water flow^{1,2} and water-related mineralogies on the surface of Mars are widespread and abundant³. Several lines of evidence, however, suggest that Mars has been cold with mean global temperatures well below the freezing point of pure water⁴. Martian climate modellers^{5,6} considering a combination of greenhouse gases at a range of partial pressures find it challenging to simulate global mean Martian surface temperatures above 273 K, and local thermal sources^{7,8} cannot account for the widespread distribution of hydrated and evaporitic minerals throughout the Martian landscape³. Solutes could depress the melting point of water^{9,10} in a frozen Martian environment, providing a plausible solution to the early Mars climate paradox. Here we model the freezing and evaporation processes of Martian fluids with a composition resulting from the weathering of basalts, as reflected in the chemical compositions at Mars landing sites. Our results show that a significant fraction of weathering fluids loaded with Si, Fe, S, Mg, Ca, Cl, Na, K and Al remain in the liquid state at temperatures well below 273 K. We tested our model by analysing the mineralogies yielded by the evolution of the solutions: the resulting mineral assemblages are analogous to those actually identified on the Martian surface. This stability against freezing of Martian fluids can explain saline liquid water activity on the surface of Mars at mean global temperatures well below 273 K.

Was early Mars warm and wet, or cold and dry? Geomorphologies derived from liquid water flowing and ponding on the surface of the planet cover most of the Martian landscape², and there is much evidence of water-related mineralogies on the surface of Mars³, implying that early Mars was wet. But several lines of evidence suggest that Mars has also been permanently cold⁴, with mean global temperatures well below the freezing point of pure water. As a way of plausibly raising its surface temperatures above 273 K, climate models consider the addition of appreciable concentrations of CO₂

(ref. 11), CH₄ (ref. 5), NH₃ (ref. 1), CO₂-CH₄-NH₃-SO₂ (ref. 12) or SO₂-H₂S (ref. 13) to the early Mars atmosphere. Yet all these model scenarios have important limitations, as follows. Although geochemical models are compatible with low partial pressures of atmospheric CO₂ in early Mars¹⁴, even a thick CO₂ atmosphere (5 bar) cannot efficiently raise the surface temperature above 273 K (ref. 6), and the greenhouse atmosphere produced by the CO₂-H₂O system would have saturated at temperatures well below 273 K (refs 5, 12). The amount of CH₄ required would imply a terrestrial-like biological source¹⁵. NH₃ would be consumed by ultraviolet photolysis in less than ten years¹⁶. Sulphur volatiles have brief residence times in the atmosphere¹⁷, with no detectable sulphur-containing gases at present. Combinations of CO₂-CH₄-NH₃-SO₂ would provide only modest warming¹². Consequently, none of these models solves the problem of liquid water on a probably very cold early Mars. Here we address this early Mars climate paradox by instead modelling the stabilization against freezing of surface liquid solutions with large concentrations of dissolved solutes.

The reduction of the freezing point of aqueous solutions is a function of chemical composition and pressure. On Mars, large evaporitic deposits of sulphates¹⁸ and chlorides¹⁹, as well as hydrated and anhydrous salts and phyllosilicates³, have been detected in numerous locations, showing that the composition of water-related minerals on the Martian surface must have derived from complex multicomponent solutions. More recently, geochemical models of early Mars aqueous solutions suggest salty rather than dilute fluids²⁰, and this salty nature of the Martian waters is a prerequisite for our model calculations (see Supplementary Information). To elucidate the thermodynamic behaviour of liquid solutions on early Mars, we have simulated the freezing and evaporation processes of fluids with a composition resulting from the weathering of basalts, as reflected in the chemical compositions at Mars landing sites²¹ (Table 1). For all the modelled compositions, the initial solution salinities in the evaporation series (starting at 275 K)

Table 1 | Percentage element mass fraction at four Martian landing sites

Element	Viking 1 (Chryse Planitia)	Pathfinder (Ares Vallis)	Opportunity (Meridiani Planum)	Spirit (Gusev crater)
Al	4.4	4.5	4.69	4.6
Ca	4.6	4.8	4.53	4.07
Cl	0.71	0.49	0.47	0.72
Cr	-	0.16	0.3	0.23
Fe	13.2	14.6	13.8	11.8
K	0.22	0.63	0.34	0.28
Mg	3.3	4.2	4.18	5.02
Mn	-	0.4	0.27	0.24
Na	-	1.0	1.58	1.88
P	-	0.42	0.32	0.49
S	2.7	2.2	2.1	3.4
Si	22.6	21.0	20.2	18.4
Ti	0.41	0.55	0.68	0.59

¹Space Science and Astrobiology Division, NASA Ames Research Center, Moffett Field, California 94035, USA. ²Departamento de Geociencias Marinas, Universidad de Vigo, Lagoas Marcosende, Vigo 36200, Spain. ³Centro de Astrobiología, CSIC-INTA, Torrejón de Ardoz 28850, Madrid, Spain. ⁴Centro de Biología Molecular Severo Ochoa, CSIC-UAM, Cantoblanco 28049, Madrid, Spain.

range between 5 and 6% (based on samples taken by the following Mars landers: 51.8 g l^{-1} Pathfinder, 54.21 g l^{-1} Viking, 54.21 g l^{-1} Spirit, 57.93 g l^{-1} Opportunity), only slightly higher than terrestrial sea water ($\sim 3.51\%$). This is because we impose an equilibrium between Si and amorphous SiO_2 , and so the excess of Si immediately precipitates as amorphous silica until under-saturation is reached. The remaining Si is ultimately involved in the precipitation of phyllosilicates. As the model system evolves, the dropping temperature and the freezing concentration increase the salinities in all cases (Table 2). Even at the high salinities reached at very low temperatures, the solutions still have a perfectly liquid appearance and behaviour, consistent with the shape and morphology of the valley networks, outflow channels and gullies seen on Mars, which suggest rapid fluvial flow rather than the slow, halting movement of thick eutectic brines with a high density and viscosity.

A certain degree of atmospheric pressure was necessary both to achieve surface temperatures that allow surface solutions to flow (otherwise global mean temperatures would have always been below 200 K, similar to those today) and to lower the vapour pressure of the liquid solutions with respect to the atmospheric pressure (so that they can exist as liquids without evaporating and becoming crusts of hydrated materials). We assumed a CO_2 atmosphere with an average pressure on the surface of 2 bar. This atmospheric partial pressure p_{CO_2} gives surface temperatures near 245 K (ref. 6), which is enough warming to enable the flow of the solutions modelled here. However, our model results are independent of the initial p_{CO_2} in the atmosphere. The same model run with an atmosphere of 10 mbar of CO_2 (which is above the triple point of water, 6.11 mbar) results in very similar outcomes in terms of liquid water stability, and shows only slight differences with respect to the sequence of mineral phase precipitation.

Our goal was to learn how a combination of different processes of evaporation and freezing affect the lowering of the freezing-point temperature of a hypothetical Martian solution. Additionally, our model calculations helped to clarify the sequence of phase formation and destabilization during the temporal evolution of the solution. We developed equilibrium models obtained by inducing lineal

Table 2 | Effect of freezing concentration (Pathfinder data)

Temperature (K)	Mass of water (kg)	Salinity (g l^{-1})	Water activity
275	1.0	51.8	0.99
263	2.171×10^{-1}	83.91	0.98
253	5.721×10^{-2}	317.0	0.97
233	2.350×10^{-2}	879.9	0.87

processes of evaporation and freezing of the liquid solutions (see Methods section). At subzero temperatures, evaporation and freezing are very efficient at increasing the ionic activity and lowering the freezing point of the solution. Our results on the evolution of residual liquid water and the phase transitions as a function of temperature are presented in Fig. 1. In all modelled scenarios, a significant fraction of liquid water remains stable at temperatures below 273 K. For example, at temperatures of 263, 250, 245 and 223 K, up to 78%, 22%, 14% and 6% of the original water reservoir remains in the liquid state, respectively. A direct comparison can be done with what is expected to occur in terrestrial sea water, where at 263 and 223 K, 20% and 0.31% of the original water would remain unfrozen²². As a result of liquid water loss through freezing and evaporation, a sequence of phase transitions dependent on the saturation equilibrium of the different components in the solution is observed. The sequence of phase precipitation and the freezing point depression both follow the same general trends for each of the landing sites' ionic composition, although minor variations can be observed by introducing changes in the initial ionic concentrations. We also studied how these ionic changes can affect the concrete behaviour of the solutions, and our results are detailed in the Supplementary Information.

In general, a very fast evaporation process would induce a lowering of the freezing point. This is because when the evaporation rate increases with respect to freezing, a smaller fraction of liquid water remains at 250 K, as some water is lost in the evaporation process and in the precipitation of hydrated phases, further concentrating the dissolved species. A fast evaporation yielded the largest drop in freezing point, down to 220 K. But, at the same time, the saturation of

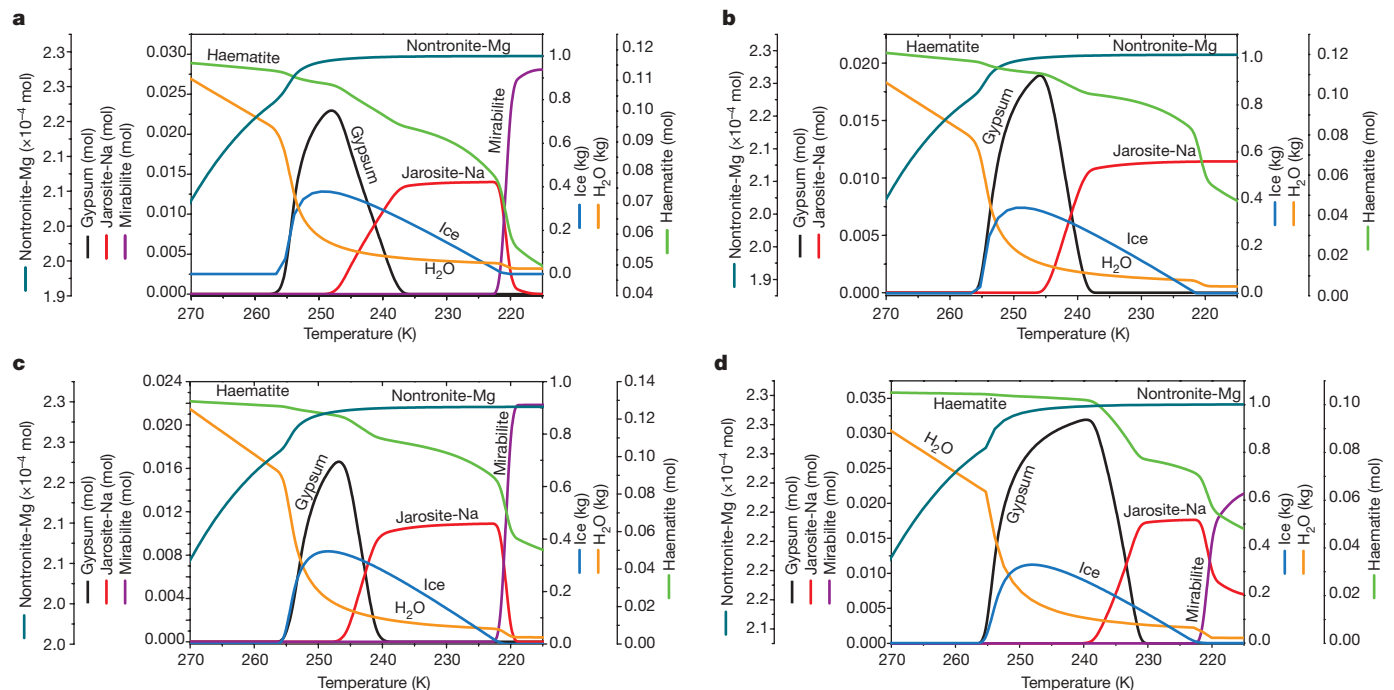


Figure 1 | Liquid water on Mars at subzero temperatures. Residual water mass, ice formation and change in ion concentrations as a function of temperature in four hypothetical Martian solutions based on data from four Mars landers (Table 1), in a model of evaporation and freezing, followed by

continuing freezing down to 215 K. Note the opposite behaviour for the different evaporitic phases (mainly gypsum versus jarosite) and their influence on the modification of the available liquid water mass. **a**, Viking; **b**, Pathfinder; **c**, Opportunity; **d**, Spirit.

many salts increases rapidly, promoting phase precipitation and therefore lowering the concentration of dissolved ions, which favours the formation of ice.

To understand evaporite composition and liquid lines of descent for Mars, we analysed the rate of ice formation in different situations, varying the relative velocity of evaporation versus freezing, and the total number of moles of water evaporated (Fig. 2). For early Mars, the preferred scenarios are those where evaporation occurred at

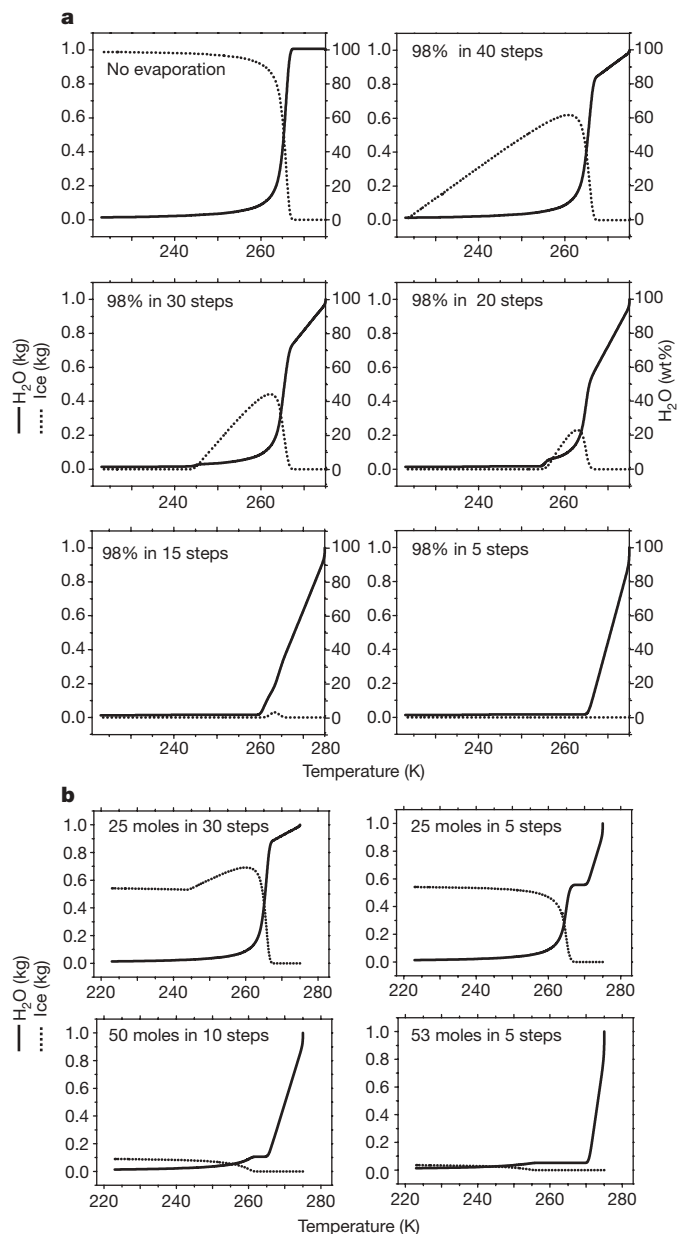


Figure 2 | Analysis of ice formation during the evaporation/freezing sequence. Evaporation of 98% of the initial liquid water mass at different velocities, related to the same freezing process, assuming that supersaturated salts were not allowed to precipitate and remained metastable. Ion composition is that in Table 1 for the Opportunity landing site. **a**, Water mass is 1 kg. The scenario of no evaporation hints at the maximum possible freezing before ice starts to form. In the other scenarios the evaporation velocity is progressively faster with respect to freezing. As the water undergoes evaporation up to 98%, the final masses of ice and water are very small. In the bottom panels, ice formation is barely observed, and the water curve (although the water mass is very small) is always over the ice curve. **b**, Different scenarios in which we varied both the relative velocity of evaporation versus freezing and the total number of moles of water evaporated.

moderate velocities (20 or 30 steps in Fig. 2a), and in which a compromise between evaporation, precipitation and freezing rates is reached, and therefore wherein the maximum amount of free liquid water at the minimum possible temperatures is attained. The minimum quantity of liquid water shown in Fig. 2 could be as voluminous as required, depending on an increase in the initial water mass in the system, and an increase in the initial ionic concentration, keeping the relative proportions in weight, which would result in brine formation at the beginning of the process. Therefore, the higher the initial water mass on Mars and its ionic concentration, the higher the mass of the water that would remain in the liquid state at very low ambient temperatures. Also, higher initial water masses will form more dilute solutions, and less initial water will create concentrated brines. Our results predict the precipitation of phyllosilicates starting at 265 K, and therefore at high water activities; while the formation of sulphates would start around 245 K, a situation in which ice would be the dominant water phase in the system. This outcome may reflect a scenario in which initial solutions favourable to the formation of phyllosilicate-type minerals in the Noachian period evolved as Mars gradually dried out into hypersaline solutions more conducive to the synthesis of sulphate-type deposits during the Late Noachian to Hesperian periods³. Alternatively, all these mineralogies could be a result of the contemporary evolution of different aqueous solutions under locally diverse environmental conditions.

Although saline solutions may not be responsible for the formation of all of the fluvial features on Mars, the geochemical analysis we present does help to explain the long-term presence of open bodies of salty water on a cold Mars. A combination of atmospheric warming by a mixture of greenhouse gases due to extensive volcanism²³ and obliquity controls on climate²⁴, resulting in surface temperatures around 245 K (ref. 6), and melting point depression of the aqueous solutions via ionic loading that stabilized the liquids at temperatures below 273 K, would have led to the flow of liquid water on the Martian surface. This model combination was only achieved during the early history of Mars, before the significant atmospheric loss that occurred by the end of the Noachian by hydrodynamic and impact escape²⁵.

However, water-shaped features have formed throughout Martian history, and may even possibly do so today to some extent²⁶. Our results are as relevant to recent processes as to early Mars, because qualitatively similar results hold when a few tens of millibars or less of CO₂ are considered. During the Amazonian period, it is more about maintaining stability against desiccation and salt crust formation, keeping the non-eutectic-acid solutions stable as liquids on the surface. Alternatively, the aqueous solutions could be extant beneath the surface at shallow depths and erupt through permafrost. In the Noachian and the Hesperian periods, less than half of the initial liquid water reservoir of Mars would have been lost through evaporation or by entrapment in the crystal structure of the precipitated hydrated salts, further supporting the idea that most of the water on the Martian surface consisted of supercooled water solutions shaping valleys and seas, partly covered by large masses of ice. In such aqueous solutions, the activity of water (a thermodynamic property of solutions that is dependent on temperature and salt concentration) would have almost never reached values below 0.95 (Table 2), and would thus be very unlikely to challenge any possible early Martian biosphere, as is proposed to have occurred at temperatures above freezing²⁰. Our results are compatible with Mars lander and orbiter data and with climate modelling, and suggest a cold and wet early Mars.

METHODS SUMMARY

The geochemical calculations were performed using the Phreeqc2.15.0 software²⁷. The model was run at decreasing temperatures from 270 to 215 K and with the following initial conditions: H₂O = 54 mol (1 kg), p_{CO_2} = 2 bar, pH = 4.0, redox potential Eh = 4.0, all sulphur as S⁶⁺, all iron as Fe³⁺. As shown in the Supplementary Information, these initial values are not determinant for the general behaviour of liquid water and ice. The evolution of the system was

analysed at specific temperature steps (40 steps, $\Delta T = 1.375$ K, see Supplementary Information), allowing solution/solid-phase equilibration at each one of these steps. For the overall evaporation and cooling calculations, the temperature dependence of the equilibrium constant was modelled using the Van't Hoff expression. The EQ3/6 database provided by the Lawrence Livermore National Laboratory²⁷ was employed for the calculations. In the version we used, the Phreeqc program implements both the ion-pairing based on the Debye–Hückel approach for the calculation of activities as the product of several fundamental constants²⁸, and the Pitzer virial-coefficient model for highly saline solutions or brines²⁹. The general system behaviour was modelled with the Debye–Hückel database to obtain the evaporation and freezing guidelines, including silicate behaviour. The final stages of the evaporation process were modelled using the Pitzer database because it is the better approach for high ionic strengths, although it has two main drawbacks: the lack of interaction parameters for aqueous Al and Si species, which precludes any calculations with aluminosilicates; and the very few data available for redox reactions. In our case, Fe^{3+} values were added to the original Pitzer database by using recent compilations^{20,30}.

Received 19 August 2008; accepted 16 March 2009.

- Sagan, C. & Mullen, G. Earth and Mars: evolution of atmospheres and surface temperatures. *Science* **177**, 52–56 (1972).
- Baker, V. R. Water and the martian landscape. *Nature* **412**, 228–236 (2001).
- Bibring, J. P. *et al.* Global mineralogical and aqueous Mars history derived from OMEGA/Mars Express data. *Science* **312**, 400–404 (2006).
- Gaidos, E. & Marion, G. Geological and geochemical legacy of a cold early Mars. *J. Geophys. Res.* **108**, doi:10.1029/2002JE002000 (2003).
- Kasting, J. F. CO_2 condensation and the climate of early Mars. *Icarus* **94**, 1–13 (1991).
- Colaprete, A. & Toon, O. B. Carbon dioxide clouds in an early dense Martian atmosphere. *J. Geophys. Res.* **108**, 5025, doi:10.1029/2002JE001967 (2003).
- Griffith, L. L. & Shock, E. L. Hydrothermal hydration of Martian crust: illustration via geochemical model calculations. *J. Geophys. Res.* **102**, 9135–9143 (1997).
- Segura, T., Toon, O. B., Colaprete, A. & Zahnle, K. Environmental effects of large impacts on Mars. *Science* **298**, 1977–1980 (2002).
- Brass, G. W. Stability of brines on Mars. *Icarus* **42**, 20–28 (1980).
- Kuzmin, R. O. & Zabalueva, E. V. On salt solutions in the Martian cryolithosphere. *Solar Syst. Res.* **32**, 187–197 (1998).
- Forget, F. & Pierrehumbert, R. T. Warming early Mars with carbon dioxide clouds that scatter infrared radiation. *Science* **278**, 1273–1276 (1997).
- Sqyres, S. W. & Kasting, J. F. Early Mars: how warm and how wet? *Science* **265**, 744–749 (1994).
- Halevy, I., Zuber, M. T. & Schrag, D. P. A sulfur dioxide climate feedback on early Mars. *Science* **318**, 1903–1907 (2007).
- Chevrier, V., Poulet, F. & Bibring, J.-P. Early geochemical environment of Mars as determined from thermodynamics of phyllosilicates. *Nature* **448**, 60–63 (2007).
- Kasting, J. F. Warming early Earth and Mars. *Science* **276**, 1213–1215 (1997).
- Kuhn, W. R. & Atreya, S. W. Ammonia photolysis and the greenhouse effect in the primordial atmosphere of the Earth. *Icarus* **37**, 207–213 (1979).
- Johnson, S. S., Mischna, M. A., Grove, T. L. & Zuber, M. T. Sulfur-induced greenhouse warming on early Mars. *J. Geophys. Res.* **113**, E08005, doi:10.1029/2007JE002962 (2008).
- Gendrin, A. *et al.* Sulfates in martian layered terrains: the OMEGA/Mars Express view. *Science* **307**, 1587–1591 (2005).
- Osterloo, M. M. *et al.* Chloride-bearing materials in the southern highlands of Mars. *Science* **319**, 1651–1654 (2008).
- Tosca, N. J., Knoll, A. H. & McLennan, S. M. Water activity and the challenge for life on early Mars. *Science* **320**, 1204–1207 (2008).
- Karunatillake, S. *et al.* Chemical compositions at Mars landing sites subject to Mars Odyssey Gamma Ray Spectrometer constraints. *J. Geophys. Res.* **112**, E08S90, doi:10.1029/2006JE002859 (2007).
- Marion, G. M. & Kargel, J. S. *Cold Aqueous Planetary Geochemistry with FREZCHEM* 102–109 (Springer, 2008).
- Phillips, R. J. *et al.* Ancient geodynamics and global-scale hydrology on Mars. *Science* **291**, 2587–2591 (2001).
- Sagan, C., Toon, O. B. & Gierasch, P. J. Climatic change on Mars. *Science* **181**, 1045–1049 (1973).
- Brain, D. A. & Jakosky, B. M. Atmospheric loss since the onset of the Martian geologic record: combined role of impact erosion and sputtering. *J. Geophys. Res.* **103**, 22689–22694 (1998).
- Fairén, A. G. *et al.* Evidence for Amazonian acidic liquid water on Mars—A reinterpretation of MER mission results. *Planet. Space Sci.* **57**, 276–287 (2009).
- Parkhurst, D. L. & Appelo, C. A. J. *User's Guide to PHREEQC (Version 2)—A Computer Program for Speciation, Batch-Reaction, One-Dimensional Transport, and Inverse Geochemical Calculations* US Geol. Surv. Wat. Resour. Invest. Rep. 99–4259 (1999).
- Debye, P. & Hückel, E. Zur theorie der electrolyte. I. Gefrierpunktniedrigung und Verwandte Erscheinungen. *Phys. Z.* **24**, 185–206 (1923).
- Pitzer, K. S. *Thermodynamics* 3rd edn (McGraw-Hill, 1995).
- Marion, G. M., Kargel, J. S. & Catling, D. C. Modeling ferrous-ferric iron chemistry with application to Martian surface geochemistry. *Geochim. Cosmochim. Acta* **72**, 242–266 (2008).

Supplementary Information is linked to the online version of the paper at www.nature.com/nature.

Acknowledgements Work by A.G.F. and A.F.D. was supported by ORAU-NPP. We thank J. Kasting and J. Kargel for reviews that significantly improved the paper.

Author Information Reprints and permissions information is available at www.nature.com/reprints. Correspondence and requests for materials should be addressed to A.G.F. (alberto.g.fairen@nasa.gov).